HHS Public Access

Author manuscript

Nat Med. Author manuscript; available in PMC 2015 July 13.

Published in final edited form as:

Nat Med. 2010 October ; 16(10): 1120–1127. doi:10.1038/nm.2213.

Dynamic regulation of cardiolipin by the lipid pump, ATP8b1, determines the severity of lung injury in experimental bacterial pneumonia

Nancy B. Ray[#1], **Lakshmi Durairaj**[#1], **Bill B. Chen**[2], **Bryan J. McVerry**[2], **Alan J. Ryan**[1], **Michael Donahoe**[2], **Alisa K. Waltenbaugh**[2], **Christopher P. O'Donnell**[2], **Florita C. Henderson**[1], **Christopher A. Etscheidt**[1], **Diann M. McCoy**[1], **Marianna Agassandian**[1], **Emily C. Hayes-Rowan**[2], **Tiffany A. Coon**[2], **Phillip L. Butler**[3], **Lokesh Gakhar**[3], **Satya N. Mathur**[1], **Jessica C. Sieren**[1], **Yulia Y. Tyurina**[4], **Valerian E. Kagan**[4], **Geoffrey McLennan**[1,5,6], and **Rama K. Mallampalli**[2,7]

[1]Departments of Internal Medicine, University of Iowa, Iowa City, IA 52242

[2]Departments of Internal Medicine, Acute Lung Injury Center of Excellence, University of Pittsburgh, Pittsburgh, PA 15213

[3]Departments of Biochemistry, University of Iowa, Iowa City, IA 52242

[4]Center for Free Radical and Antioxidant Health, Department of Environmental and Occupational Health, University of Pittsburgh, Pittsburgh, PA 15219

[5]Department of Radiology, University of Iowa, Iowa City, IA 52242

[6]Department of Biomedical Engineering, University of Iowa, Iowa City, IA 52242

[7]Veteran's Affairs Pittsburgh Healthcare System, Pittsburgh, PA 15206

[#] These authors contributed equally to this work.

Abstract

Pneumonia remains the leading cause of infectious deaths and yet fundamentally new conceptual models underlying its pathogenesis have not emerged. Patients and mice with bacterial pneumonia have marked elevations of cardiolipin in lung fluid, a rare, mitochondrial-specific phospholipid that potently disrupts surfactant function. Intratracheal cardiolipin in mice recapitulates the clinical

[*]**Address Correspondence to**: Rama K. Mallampalli, M.D., Department of Internal Medicine, PACCM, NW628 Montefiore, 3459 Fifth Avenue, Pittsburgh, PA 15213, Telephone: 412-692-2112, Fax: 412-692-2260, mallampallirk@upmc.edu.

Author Contributions

N.B.R designed and executed CL-ATP8b1 binding, in vitro imaging, immunological studies, and wrote the manuscript. L.D. edited the manuscript, conducted the human studies. B.B.C. performed in vitro (CL uptake, biochemical and molecular) experiments, and all animal studies. B.J.M. and M.D. contributed to human studies and statistical analyses. A.K.W., T.A.C., M.A., P.L.B., F.C.H., S.N.M. performed in vitro studies. A.J. R. and C.P.O. performed mouse studies. D.M., E.H-R., and C.E. conducted CL analysis. L.G. conducted surfactant studies. J.C.S. and G.M. designed and conducted in vivo imaging. V.E.K. designed and executed mass spectrometry of CL with assistance from Y.Y.T. and V.E.K provided editorial suggestions. R.K.M. revised the manuscript and directed the study.

Competing financial interests

The authors declare no competing financial interests.

phenotype of pneumonia including impaired lung mechanics, modulation of cell survival and cytokine networks, and lobar consolidation. We have identified and characterized the activity of a novel cardiolipin transporter, ATP8b1, a mutant version of which is associated with severe pneumonia in humans and mice. ATP8b1 bound and internalized cardiolipin from extracellular fluid via a basic residue-enriched motif. Administration of cardiolipin binding motif peptide or ATP8b1 gene transfer in mice lessened lung injury and improved survival. The results unveil a new paradigm whereby ATP8b1 is a cardiolipin importer but its capacity to remove cardiolipin from lung fluid is exceeded during inflammation or ATP8b1 inefficiency. This discovery opens the door for new therapeutic strategies directed at modulating cardiolipin levels or its molecular interactions in pneumonia.

Introduction

Pneumonia is the leading cause of death in the US from infectious causes and it is second (only to childbirth) for hospital admission[1]. Thus, it remains a major cause of morbidity and contributes significantly to healthcare costs in both the community and hospitalized patients. The pathobiology of bacterial pneumonia after infection with highly virulent pathogens (Streptococcus pneumoniae, Staphylococcus aureus, H. influenzae and *E. coli*) typically involves neutrophilic lung infiltration and a robust host immune response leading to severe ventilatory abnormalities. Several microbial virulence and host factors partake in the progression of pulmonary injury [2]. Despite decades of intensive study, there has been a lack of fundamentally new biological mechanisms that have emerged with regard to the pathobiology of bacterial pneumonia. Consequently, there has been an over-reliance on the use of broad spectrum antibiotics in severe infection with the emergence of multi-drug resistant strains.

In the process of identifying mediators of pulmonary infection, we analyzed patients with bacterial pneumonia and discovered elevated levels of the phospholipid, cardiolipin (CL) in lung fluid. CL is typically a minor component of pulmonary lavage fluid and comprises only ~1-2% of alveolar surfactant, a surface-tension lowering material enriched with phosphatidylcholine and key apoproteins that is secreted into the airways by type II alveolar epithelia [3]. Elevated CL levels are seen in lung injury models [4,5]. However, the biological significance and mechanisms for changes in CL content remains enigmatic. The findings of very low CL levels in lung fluid under native conditions suggest the existence of control mechanisms that tightly regulate CL availability within the airways or extracellular fluid.

One population at increased risk for pneumonia includes patients with progressive familial intrahepatic cholestasis type 1 (PFIC1, or Byler Disease) [6,7]. Pneumonia and respiratory symptoms were seen in 13% and 26% of PFIC1 patients [6,8]. PFIC1 patients have mutations in the P-type ATPase transmembrane lipid pump, ATP8b1. Type 4 P-type ATPases maintain lipid balance by translocating phospholipids from the outer to inner leaflets of membrane bilayers. ATP8b1 translocates phosphatidylserine (PS) from the outer to inner membrane in cells, is highly expressed in apical epithelial membranes, and is present in various human tissues [7]. The observation that patients with PFIC1 are prone to respiratory infection coupled with the ability of ATP8b1 to transport phospholipids across cellular membranes led us to

hypothesize that ATP8b1 is an authentic CL import protein. To test this hypothesis, we used ATP8b1 defective mice that harbor a prototypic PFIC1 mutation (G308V) observed in patients with severe PFIC1.

In this study, we discovered that CL is elevated in lung fluid of patients with pneumonia and that the lipid is a highly potent surfactant inhibitor that disrupts lung structure and function. The abundance of CL in lung fluid is regulated by ATP8b1, which effectively binds and internalizes the lipid in lung epithelia via domain specific interactions. ATP8b1 mutant mice have elevated CL levels in lung fluid and were prone to bacterial induced lung injury. These results provide a novel conceptual model for bacterial pneumonia where ATP8b1 serves as a molecular transporter that evacuates an injurious bioactive lipid from distal airways to preserve pulmonary homeostasis.

Results

CL is elevated in pneumonitis

CL was quantitated in tracheal aspirates from critically ill subjects with non-pulmonary illnesses (*n*=five), clinically diagnosed pneumonia (*n*=17), or congestive heart failure (CHF) (*n*=six, Supplementary Table I). Control patients with non-pulmonary illnesses included those requiring mechanical ventilation for liver failure, hemolysis elevated liver enzymes low platelets (HELLP) syndrome, Guillain-Barre syndrome, renal failure, and gastrointestinal tract bleeding. Subjects with pneumonia were identified as having new or changing radiographic pulmonary infiltrates, increasing sputum quantity or change in sputum character, and clinical features such as fever, elevated white blood cell count and hypoxemia without dependence upon sputum culture results or distinction between community or hospital acquisition. No bacterial growth was detected in 39% (7/17) of subjects with pneumonia while tracheal aspirates grew *Streptococcus pneumoniae* in four subjects, *Pseudomonas aeruginosa* and *Staphylococcus aureus* in three subjects each, and *Haemophilus influenza* in one subject. 90% (26/28) of all subjects were on broad-spectrum antibiotics on the day of tracheal aspirate collection (Supplementary Table. 1). Subjects with pneumonia had significantly higher levels of CL (median=12.9 Mol%) in tracheal aspirates compared to subjects with non-pulmonary diagnoses (~9.7 fold) or CHF (~6 fold, Kruskal-Wallis *P*=0.0007, Fig. 1a). Importantly, CL levels did not correlate with culture status, bacterial pathogen, duration of mechanical ventilation, gender, or age (Supplementary Fig. 1).

Mice were also infected with strains of *H. influenzae* or *E. coli* that cause pneumonia [9,10]. Bronchoalveolar lavage (BAL) fluid from infected mice had greater levels of CL than BAL isolated from uninfected mice (Fig. 1b). To assess if elevated CL levels were due to reduced cellular uptake, primary mouse type II lung epithelia were cultured with [^{3}H] CL. Infection with *H. influenzae* or *E. coli* resulted in significantly reduced cellular uptake of [^{3}H] CL (Fig. 1c). Thus, CL is increased in lung fluid of both patients and animal models with pneumonitis and this may be due to decreased epithelial uptake of the phospholipid.

CL impairs lung structure, function, and cell viability

Phospholipids (CL, LPC [lysophosphatidylcholine], PS [phosphatidylserine]) were incorporated into Infasurf (a commercial apoprotein containing surfactant) to generate lipid vesicles that were used to assay surface-tension (Fig. 2a). Lipids were also extracted from Infasurf to generate protein-deficient preparations that were reconstituted with phospholipids for testing (Fig. 2b). Unlike PS, increasing CL concentrations (> 3 Mol%) resulted in increased surface-tension. CL impaired surface-activity to a greater extent than LPC, a positive control [11]. These adverse effects of CL were more pronounced when testing lipid extracts devoid of surfactant-associated apoproteins (Fig. 2b). Mice given intratracheal (i.t.) CL had significantly decreased lung compliance and increased elastance and resistance compared to controls (Fig. 2c-f). CL also increased BAL protein concentration (Supplementary Fig. 2a), differentially altered surfactant proteins (Supplementary Fig. 2b), reduced γ-interferon and IL-2 and increased IL-10 (Supplementary Fig. 2c,d), but did not affect the distribution of various inflammatory cells (Supplementary Fig. 2e) *in vivo*. Thus, CL in lung fluid adversely affects lung mechanics by greatly impairing surfactant activity. The lipid also modulates expression of cytokine networks that could impact lung stability.

Mice were subjected to live imaging of lungs by micro CT scanning (Fig. 3a). Compared to diluent, mice given CL (50 nmol) had more prominent markings in parenchyma with scattered patchy areas of alveolar consolidation (arrows). These abnormalities were more severe after high doses of CL. Histological analysis identified areas of alveolar infiltration and appearance of foamy cells within alveoli (Fig. 3a, lowest, mid panel, arrows). High dose CL produced edema and disruption of alveolar lining cells (Fig. 3a, lower right panels, Fig. 3b,c) that contributed to fatality of mice within 2-3 h. CL activated the apoptotic program in cells (Fig. 3d, left) and in tissue (Fig. 3d, right panel) and it decreased cell viability (Fig. 3e) and increased cell toxicity (Fig. 3f).

ATP8b1 is an alveolar epithelial CL importer

Because CL is internalized by alveolar cells, we hypothesized that cells would express an import protein that regulates CL levels in lung fluid. ATP8b1 was a candidate protein as it internalizes phospholipids and patients with ATP8b1 defects are prone to pneumonia [8]. Type II cells had high levels of ATP8b1 compared to macrophages or fibroblasts (Supplementary Fig. 3a, [inset]), ATP8b1 expression was regulated (Supplementary Fig. 3b), and it exhibited surface expression (Supplementary Fig. 3c). Lentiviral ATP8b1 expressing cells had higher levels of mRNA and protein expression coupled with a robust increase in the uptake of fluorescent (nitrobenzoxadiazole [NBD]) labeled NBD-CL or NBD-PS (positive control) compared to non-transduced cells (Supplementary Fig. 3d, Fig. 4a, b). ATP8b1 overexpressing cells had greater fluorescence on both the cell surface and inside the cells, indicating that the NBD-CL was located on the plasma membrane and within the cytoplasm. Although ATP8b1 internalized CL, it did not enhance GFP-labeled *E. coli* uptake (Supplementary Fig. 3e).

Mice were also administered adenovirus (Ad5) expressing ATP8b1 or empty adenovirus prior to *E. coli* infection. Mice infected with *E. coli* at 1×10^6 CFU/mouse cleared the pathogens by 48 h of analysis. These mice exhibited decreased BAL macrophages with a

neutrophilic infiltrate typical of pneumonia, a profile not affected by Ad5-ATP8b1 gene transfer (Supplementary Fig. 4a). Ad5 alone or Ad5 encoding ATP8b1 tended to have high BAL protein concentrations associated with release of pro-inflammatory cytokines after bacterial infection (Supplementary Fig. 4b,c). ATP8b1 gene delivery before *E. coli* infection also reduced collectins, surfactant protein A (SP-A) and surfactant protein D (SP-D), but did not affect surfactant protein B (SP-B), the latter essential for surfactant activity (Supplementary Fig. 4d). Importantly, ATP8b1 gene delivery effectively increased pump levels, reduced CL levels, and reversed *E. coli* induced impairment of lung mechanics (Fig. 4c,d, Supplementary Fig. 4e) compared to infected mice given Ad5. ATP8b1 gene transfer did not reduce apoptosis after bacterial infection (Fig. 4e). Thus, the primary mechanism for beneficial effects of increased ATP8b1 expression is via reduced CL availability, thereby preserving surfactant function and improving lung mechanics. These effects were sufficient to result in increased survival of mice (Fig. 4f).

Additional loss-of-function studies were performed using siRNA and ATP8b1 mutant mice that harbor a single amino acid substitution ($Gly^{308} \rightarrow Val$) resulting in an apparent defect in PS importability [12,13]. ATP8b1 siRNA produced a significant decrease in CL uptake and selectively reduced immunoreactive ATP8b1 compared to control RNA (Fig. 5a). HaeIII restriction digest fragment patterns were used to genotype mutant, wild-type, and heterozygous mice revealing that mutants lacked 500 bp and 300 bp digest fragments (Fig. 5b). We detected low level ATP8b1 expression in mutant liver and lung compared to wild-type tissues (Fig. 5c). ATP8b1 mutant mice had significantly higher BAL CL versus wild-type littermates (Fig. 5d). Consistent with ATP8b1's inability to alter bacterial uptake, bacterial loads did not differ between ATP8b1 mutant and wild-type mice (Supplementary Fig. 5a). Both ATP8b1 defective and wild-type littermates exhibited no differences in BAL protein content (Supplementary Fig. 5b), wet/dry lung weight ratios (Supplementary Fig. 5c), or cellular inflammation (Supplementary Fig. 5d) after infection. Interestingly, ATP8b1 defective mice exhibited a blunted cytokine response to Th1 cytokines (interferon-γ, TNF-α, IL-β) compared to wild-type littermates after *E. coli* infection (Supplementary Fig. 6a,b) which may be secondary to increased expression of SP-A and SP-D (Supplementary Fig. 6c)[14,15]. Primary type II cells isolated from ATP8b1 mutant mice exhibited a blunted response with regard to NBD-CL uptake compared to cells isolated from wild-type littermates (Fig. 5e). Mutant mice also had impaired biophysical properties compared to wild-type mice particularly following *E. coli* infection (Figs. 5f,g, Supplementary Fig. 6d). Although mutant mice also were more prone to apoptosis (Fig. 5h), there was no significant difference in mortality between ATP8b1 mutant and wild-type mice with infection (Fig. 5i). Collectively, these studies strongly suggest that ATP8b1 is a *bona fide* alveolar epithelial CL import pump.

CBD peptide blocks CL uptake and lung injury

We mapped the ATP8b1-CL binding domain (CBD). Synthesized deletion mutants (Supplementary Fig. 7a,b) were reacted with fifteen lipids pre-spotted onto hydrophobic lipid strips (Supplementary Fig. 7c). Using this system, FL ATP8b1 and specific mutants were observed to bind CL and also sulfatide (Supplementary Fig. 7c). C–terminal truncation mutants containing only the first 810 or 771 residues did not bind CL suggesting that a CBD

resides between residues 810 to 850 within ATP8b1. This was confirmed by testing a fragment (residues 771-850) that was sufficient for CL binding indicating that a novel CBD resides within the ATP8b1 carboxyl-terminus (Supplementary Fig. 7c).

A cDNA encoding the putative CBD was fused to GST, for expression of purified protein from cells. Cells cultured with GST-CBD peptide exhibited an 83% decrease in [^{3}H] CL uptake versus GST peptide alone (Fig. 6a). Mice infected with or without *E. coli* and given CBD peptide compared to vehicle exhibited a significantly increased proportion of macrophages and modestly reduced protein content and BAL neutrophils (Supplementary Fig. 8a,b). Importantly, CBD peptide profoundly reduced TNF-α, and IL-β levels and significantly reduced GM-CSF levels after bacterial infection (Fig 6, Supplementary Fig. 8c). CBD peptide did not alter surfactant apoproteins nor the degree of apoptosis (Supplementary Fig. 9a,c). Infected mice given vehicle exhibited impaired lung mechanics, effects that were reversed after CBD peptide administration (Fig. 6b,c,d, Supplementary Fig. 9b). These beneficial effects of CBD peptide on pulmonary homeostasis led to significantly improved survival in mice (Fig. 6f). Thus, the CBD within ATP8b1 is functional with regard to substrate binding and this peptide exerts biological effects in concert with its activity in antagonizing actions of CL *in vivo*.

Discussion

Pneumonia remains a major public health challenge and a major cause of intensive care unit admission. Antimicrobial agents remains the cornerstone of therapy for bacterial pneumonia but few non-antibiotic therapies have emerged that impact outcomes of patients with severe infection. The data here provides a new conceptual model involving CL as mediator of pneumonia and its trafficking by ATP8b1. We show that CL is significantly elevated both in human subjects with pneumonia and in mice infected with bacterial pathogens. CL potently impairs lung mechanics by antagonizing surfactant function leading to high surface-tension pulmonary edema (Figs. 2a, Fig.3b,c)[16,17]. CL was also observed to disrupt pulmonary architecture and reduce epithelial cell viability. Our finding that adverse effects of CL are antagonized by CL binding peptide suggest that future studies might entail use of small molecule modifiers that regulate CL availability as novel non-antibiotic treatment strategies for patients with pneumonia.

Because CL is an apoptotic cell surface marker and a constituent of bacterial membranes, it is plausible that its release in lung fluid during pneumonia represents infections having very high bacterial burdens. CL content in some bacterial envelopes, such as *E. coli*, is very high but it is undetectable in *H. influenzae* membranes [18,19]. Yet both pathogens reduced CL uptake (Fig. 1c) and increased CL concentrations (Fig. 1b) suggesting other mechanisms for its origin. One possibility is that CL, normally exclusively present within the inner mitochondrial membrane, is released from dying host cells, particularly during execution of intrinsic mitochondria-dependent apoptosis. Early in the programmed cell death, CL transmigrates to the outer mitochondrial membrane [20] and can also reach the outer leaflet of the cell's plasma membrane [21] where it could be readily integrated in surfactant. Because molecular signatures of CL species differ between mammalian cells and bacterial membranes, we examined the source of CL in pneumonia patients (Supplementary Fig.10a)

and mice infected with *E. coli* (Supplementary Fig. 10b). Indeed, ESI-MS spectra of CLs obtained from human and mouse samples demonstrate that CL originates from mammalian cells. Hence mitochondria-specific mammalian species of CL - not bacterial - were found in lung fluid samples. These results do not totally exclude a bacterial origin, as bacterial CL elevation in fluid may be transient or prokaryotic organisms might utilize host cell mitochondrial CL that is incorporated into bacterial membranes. Last, host (type II cell) apoptosis could lead to reduced surfactant production independently from effects of CL.

CL is highly effective in inhibiting surfactant activity. CL was twice as potent as lysophosphatidylcholine, a gold standard reference [22]. Optimal surfactant activity depends on tight molecular packing of the major surfactant phospholipid, dipalmitoyl-phosphatidylcholine (DPPC), within a film at the air-surface interface. CL's ability to block surface-tension lowering by DPPC would be predicted because of its bulky molecular structure that would impede DPPC packing. It is difficult to equate CL concentrations in human tracheal aspirates (Fig. 1a) with pathophysiologic levels of CL incorporated into the DPPC film in human BAL fluid. This is because of significant issues of recovery, sample dilution, and tight binding of CL with mitochondrial proteins reducing its extraction [23]. However, inhibitory actions of CL were seen even at very low concentrations (~ 2 Mol%) (Fig. 2b) using CL liposomes devoid of surfactant apoproteins [3]. Thus, surfactant proteins may protect against CL inhibition and adverse CL effects may be more pronounced when surfactant proteins are depleted [24]. When CL was added as liposomes with apoproteins, surface-tension was markedly elevated (Fig. 2a). Here, higher concentrations of CL (at 5-20 Mol%) as seen in pneumonia patients are needed to impair surface-activity. The data suggest that CL concentrations that impair surface-activity are within the pathophysiologic range. These observations need to be confirmed in larger studies adjusted for important factors (smoking status, illness severity, lung compliance, and comorbidities) as the current results in tracheal aspirates are associative and lack important measures such as cell counts and proteins, and were not adjusted for dilution. The use of BAL or Mini-BAL may further strengthen these associations by improving the accuracy of pneumonia diagnosis and adjusting for inflammatory markers. Subgroup CL analysis (e.g. alveolar hemorrhage and stages of acute lung injury) are also essential in understanding these associations. Serial measurements during mechanical ventilation may better link tracheal colonization and resolving inflammation with CL levels in tracheal aspirates.

Alveolar cells harbor active transport mechanisms to maintain very low CL concentrations typically seen in human lavage fluid [25,26]. Evidence in support of ATP8b1 as an authentic CL import protein include that (i) ATP8b1 binds CL within a highly charged inter-transmembrane domain loop, (ii) *in vivo* administration of a peptide containing this putative CBD signature or Ad5-ATP8b1 gene transfer lowers CL levels coupled with reduced lung injury severity, and (iii) ATP8b1 defective mice have increased CL levels and are vulnerable to bacterial-induced lung injury. The data might suggest that CL elaborated during pulmonary infection exceeds the substrate binding capacity by ATP8b1. Here, bacteria could down-regulate ATP8b1 expression, mask the CL-binding pocket by inducing ATP8b1 conformational changes, or reduce pump catalytic function. In this regard, *H. influenzae* triggers ATP8b1 degradation and ubiquitination (Supplementary Fig. 11). Presumably,

redundant mechanisms for CL import are insufficient as ATP8b1 mutant mice displayed sensitivity to pulmonary sepsis. Other related ATP-driven pumps, ATP8a1 and ATP11a, did not transport CL (Supplementary Fig. 12).

These studies are the first demonstrating cellular uptake of CL via protein binding. The ATP8b1-CL binding domain (CBD) was mapped to a 40 residue motif within a predicted inter-transmembrane loop [2728] (Supplementary Fig. 7). This loop contains several regulatory elements including a D554N missense mutation seen in PFIC1 patients [28]. As PFIC1 patients have a higher incidence of respiratory symptoms there may be additional polymorphisms within the CBD that predisposes patients to infection. Administration of CBD peptide in mice significantly lessened pulmonary impairment after infection suggesting that the molecular interactions between the ATP8b1 motif and CL are preserved *in vivo*. Manipulation of CL appears to modulate the inflammatory response (Supplementary Fig. 8, Fig.6) and CL inhibits key cell survival pathways, effects blocked by CBD peptide (Supplementary Fig.13). Thus, alveolar CL and the peptide appear to exert immunomodulatory actions that could affect resolution of pulmonary injury. These results might eventually serve as a springboard to generate drug therapies to sequester or enhance clearance of injurious CL in pneumonia.

Methods

Human samples

The study was approved by respective institutional review boards. After obtaining informed consent, tracheal aspirates were collected using an inline suction catheter without saline dilution. Patients were diagnosed with pneumonia (clinical diagnosis and confirmed with infiltrates on chest x-ray), CHF (clinical diagnosis and confirmed with pulmonary edema on chest x-ray) and included control subjects who were intubated for non-pulmonary illnesses (normal chest x-ray). Aliquots were sent for routine cultures.

Cells

Mouse lung epithelial (MLE) cells were cultured as described [32]. Cells were serum starved for 24 h then exposed to 120 nmol/ml Infasurf, PC liposomes, or CL (5-15 Mol %). Mouse alveolar type II cells, macrophages, and fibroblasts were isolated as described [32]. Cell viability was determined using the CellTiter-Glo Luminescent Cell Viability assay (Promega). LDH release was assayed by monitoring the NAD-NADH reaction at a 340 nm wavelength.

[^{3}H]-CL uptake

[^{3}H]- CL (Moravek Biochemicals, Inc.) was reconstituted in liposomes using Infasurf (Forest Pharmaceuticals Inc.) and added to medium for 2 h at 37 °C. Cellular uptake was terminated by washing with serum-free cold media twice and 2% fatty acid free BSA in PBS. Lipids were extracted (1 ml hexane:isopropanol (3:2, v/v)), solvents dried, and radioactivity (dpm) in lipids measured by scintillation counting.

Adenoviral expression

FL ATP8b1 was amplified from an expression clone in pcDNA3.1D/V5-His using a forward and reverse primer with engineered EcoRI or SpeI restriction sites, respectively. The amplified product was directionally cloned into the EcoRI and BamHI sites of the adenovirus shuttle plasmid, pacAd5 CMV K-NpA. An adenovirus expression vector including V5-FL ATP8b1 was produced by the University of Iowa Gene Transfer Vector Core [33].

Mice

C57BL/6 mice (Jackson Laboratories) were used according to Institutional Animal Care and Use Committee approved protocols. *E. coli* (ATCC 25922) (1×10^6 CFU (colony forming units)) was administered intratracheally (i.t). Mice were infected i.t. (2×10^8 CFU, nontypable *H. influenzae*) or given agarose [29] for 72 h prior to lung lavage. For adenoviral gene transfer, mice received 2.5×10^8 PFU (plaque forming units) i.t. and 24 h later given *E. coli* for 48 h. Mice were mechanically ventilated with a FlexiVent system [34]. Mice were also given *E. coli,* ventilated, and 48 h later diluent or ATP8b1 CBD peptide was delivered into lungs using a microsprayer aerosolizer. After 10 min, biophysical measurements were taken. For assay of lung edema, mice received CL (15 mM in 50 μl saline i.t.) or vehicle (50 μl saline). Evan's Blue dye (40 μg/g in 100 μl saline) was injected intravenously via the femoral vein 30 min later, BAL was obtained, Dye concentration was determined using a spectrophotometer at a wavelength of 620 nm. For wet/dry weights lungs were removed, blotted, and placed in tared weigh boats and weighed. The lungs were then dried (24 h at 60 °C) and weighed again.

Fluorescent microscopy

Cells were plated (35 mm culture dishes) and incubated with NBD-CL and NBD-PS (25 °C), and then immediately incubated at 4 °C for 5 min prior to washing with medium. Fluorescence was detected using an epifluorescent microscope (Olympus).

Lentiviral stable cell line

Lentivirus expressing ATP8b1 was produced using pLenti6/V5-DEST by the University of Iowa Gene Transfer Vector Core. Cells were transduced with a final concentration of 4 μg/ml of polybrene (Sigma) in MEM-F12, at a multiplicity of transduction of 10:1. A final concentration of 2.5 μg/ml blasticidin (Invitrogen) was used to select for transduced cells.

NBD-lipid uptake

NBD-labeled phosphatidylserine (PS) (Avanti Polar Lipids, Inc.) and NBD- CL (Invitrogen) were incubated with cells for 30 min at 37 °C. Lipids were extracted twice with 1 ml hexane:isopropanol (3:2, v/v). The solvents were evaporated under nitrogen and lipids dissolved in methanol. The fluorescence of NBD-labeled lipids was measured (excitation and emission at 460/530 nm) and quantitated using standard curves for known amounts of the NBD-labeled lipids.

NAO-CL quantitation

Lipids were extracted [35,36] and CL bound to fluorescent nonyl acridine orange (NAO) was quantitated using a spectrophotometer measuring NAO excitation and emission (494/530 nm) using standard curves [37]. Values were normalized for total phospholipid phosphorus [38] and expressed as ratios (Mol%) of phosphorus (nmol) in CL to total phospholipid (nmol) within samples.

Lipid overlay

Lipid strips (Echelon Biosciences, Inc.) were incubated with translation products in TTBS buffer with 1% fatty acid-free BSA. Strips were washed extensively and radiolabeled protein was detected with V5 antibody using immunoblotting.

ATP8b1 knockdown

A549 alveolar type II (ATII) cells were transfected twice with 2 μg of ATP8b1 ON TARGET plus SMARTpool siRNA or ON-TARGET plus Non-targeting Pool control siRNA (Dharmacon) for 48 h using Fugene 6 prior to harvest.

Statistical Analysis

We used a Prism program version 4.03 (GraphPad Software, Inc.) using an ANOVA or unpaired t test with $P<0.05$ indicative of significance. Kaplan Meier survival estimates were done using SAS version 9.2 (SAS institute). For human data, nonparametric testing using a Kruskal-Wallis and post hoc Wilcoxon rank sum test was performed.

Supplementary Material

Refer to Web version on PubMed Central for supplementary material.

Acknowledgements

The authors thank Dr. Mark E. Anderson, Dr. Michael J. Welsh, Dr. Joseph Zabner, and Dr. Mark Gladwin for critical review of the manuscript and helpful suggestions. ATP8b1$^{G308V/G308V}$ 129S1/SvlmJ mutant [13] mice were a generous gift from Dr. L. Bull (University of California, San Francisco). Nontypable *Haemophilus influenza* strain 12 bacteria was kindly provided by Dr. D. Look (University of Iowa) [29]. Antibodies to ATP8b1 were generous gifts from Dr. D. Ortiz, (Tufts University) [30] and Dr. M. Ananthanarayanan (Mount Sinai School of Medicine, NY) [31] . This work was supported by a Merit Review Award from the Department of Veteran's Affairs, and US National Institutes of Health R01 Grants HL068135, HL080229, HL081784, HL096376, HL097376, and HL098174 (to RKM), and K23 HL075402, and U01 HL102288 (to LD).

References

1. Farr BM. Prognosis and decisions in pneumonia. N Engl J Med. 1997; 336:288–289. [PubMed: 8995094]
2. Kadioglu A, Weiser JN, Paton JC, Andrew PW. The role of Streptococcus pneumoniae virulence factors in host respiratory colonization and disease. Nat Rev Microbiol. 2008; 6:288–301. [PubMed: 18340341]
3. Rooney SA, Young SL, Mendelson CR. Molecular and cellular processing of lung surfactant. FASEB Journal. 1994; 8:957–967. [PubMed: 8088461]
4. Liau DF, Barrett CR, Bell AL, Cernansky G, Ryan SF. Diphosphatidylglycerol in experimental acute alveolar injury in the dog. J Lipid Res. 1984; 25:678–683. [PubMed: 6481242]

5. Ksenzenko SM, et al. Effect of triiodothyronine augmentation on rat lung surfactant phospholipids during sepsis. J Appl Physiol. 1997; 82:2020–2027. [PubMed: 9173972]
6. Whitington PF, Freese DK, Alonso EM, Schwarzenberg SJ, Sharp HL. Clinical and biochemical findings in progressive familial intrahepatic cholestasis. J Pediatr Gastroenterol Nutr. 1994; 18:134–141. [PubMed: 7912266]
7. Bull LN, et al. A gene encoding a P-type ATPase mutated in two forms of hereditary cholestasis. Nat Genet. 1998; 18:219–224. [PubMed: 9500542]
8. Pawlikowska L, et al. Differences in presentation and progression between severe FIC1 and BSEP deficiencies. J Hepatol. 2010
9. Mizgerd JP. Acute lower respiratory tract infection. N Engl J Med. 2008; 358:716–727. [PubMed: 18272895]
10. Dullforce P, Sutton DC, Heath AW. Enhancement of T cell-independent immune responses in vivo by CD40 antibodies. Nat Med. 1998; 4:88–91. [PubMed: 9427612]
11. Grossmann G, et al. Experimental neonatal respiratory failure induced by lysophosphatidylcholine: effect of surfactant treatment. J Appl Physiol. 1999; 86:633–640. [PubMed: 9931201]
12. Paulusma CC, et al. Atp8b1 deficiency in mice reduces resistance of the canalicular membrane to hydrophobic bile salts and impairs bile salt transport. Hepatology. 2006; 44:195–204. [PubMed: 16799980]
13. Pawlikowska L, et al. A mouse genetic model for familial cholestasis caused by ATP8B1 mutations reveals perturbed bile salt homeostasis but no impairment in bile secretion. Hum Mol Genet. 2004; 13:881–892. [PubMed: 14976163]
14. Borron P, et al. Surfactant-associated protein A inhibits LPS-induced cytokine and nitric oxide production in vivo. Am J Physiol Lung Cell Mol Physiol. 2000; 278:L840–847. [PubMed: 10749762]
15. Yamazoe M, et al. Pulmonary surfactant protein D inhibits lipopolysaccharide (LPS)-induced inflammatory cell responses by altering LPS binding to its receptors. J Biol Chem. 2008; 283:35878–35888. [PubMed: 18990700]
16. Kennedy JI Jr. High alveolar surface tension pulmonary edema--relationship to adult respiratory distress syndrome. J. Thor. Cardiovasc. Surg. 1990; 100:145–146.
17. Albert RK, Lakshminarayan S, Hildebrandt J, Kirk W, Butler J. Increased surface tension favors pulmonary edema formation in anesthetized dogs' lungs. J. Clin. Invest. 1979; 63:1015–1018. [PubMed: 447823]
18. Koppelman CM, Den Blaauwen T, Duursma MC, Heeren RM, Nanninga N. Escherichia coli minicell membranes are enriched in cardiolipin. J Bacteriol. 2001; 183:6144–6147. [PubMed: 11567016]
19. Sutrina SL, Scocca JJ. Phospholipids of Haemophilus influenzae Rd during exponential growth and following the development of competence for genetic transformation. J Gen Microbiol. 1976; 92:410–412. [PubMed: 1082925]
20. Kagan VE, et al. Cytochrome c acts as a cardiolipin oxygenase required for release of proapoptotic factors. Nat Chem Biol. 2005; 1:223–232. [PubMed: 16408039]
21. Sorice M, et al. Cardiolipin on the surface of apoptotic cells as a possible trigger for antiphospholipids antibodies. Clin Exp Immunol. 2000; 122:277–284. [PubMed: 11091286]
22. Wang Z, Notter RH. Additivity of protein and nonprotein inhibitors of lung surfactant activity. Am. J. of Respir. Crit. Care Med. 1998; 158:28–35. [PubMed: 9655703]
23. Ritov VB, Menshikova EV, Kelley DE. Analysis of cardiolipin in human muscle biopsy. J Chromatogr B Analyt Technol Biomed Life Sci. 2006; 831:63–71.
24. Benarafa C, Priebe GP, Remold-O'Donnell E. The neutrophil serine protease inhibitor serpinb1 preserves lung defense functions in Pseudomonas aeruginosa infection. J Exp Med. 2007; 204:1901–1909. [PubMed: 17664292]
25. McCormack FX, King TE Jr. Voelker DR, Robinson PC, Mason RJ. Idiopathic pulmonary fibrosis. Abnormalities in the bronchoalveolar lavage content of surfactant protein A. Am Rev Respir Dis. 1991; 144:160–166. [PubMed: 2064123]
26. Hughes DA, Haslam PL. Changes in phosphatidylglycerol in bronchoalveolar lavage fluids from patients with cryptogenic fibrosing alveolitis. Chest. 1989; 95:82–89. [PubMed: 2909359]

27. Jirsa M, et al. Indel in the FIC1/ATP8B1 gene-a novel rare type of mutation associated with benign recurrent intrahepatic cholestasis. Hepatol Res. 2004; 30:1–3. [PubMed: 15341767]
28. van Mil SW, Klomp LW, Bull LN, Houwen RH. FIC1 disease: a spectrum of intrahepatic cholestatic disorders. Semin Liver Dis. 2001; 21:535–544. [PubMed: 11745041]
29. Frick AG, et al. Haemophilus influenzae stimulates ICAM-1 expression on respiratory epithelial cells. J Immunol. 2000; 164:4185–4196. [PubMed: 10754314]
30. Ujhazy P, et al. Familial intrahepatic cholestasis 1: studies of localization and function. Hepatology. 2001; 34:768–775. [PubMed: 11584374]
31. Frankenberg T, et al. The membrane protein ATPase class I type 8B member 1 signals through protein kinase C zeta to activate the farnesoid X receptor. Hepatology. 2008; 48:1896–1905. [PubMed: 18668687]
32. McCoy DM, Fisher K, Ryan AJ, Mallampalli RK. Transcriptional regulation of lung cytidylyltransferase in developing transgenic mice. Am J Respir Cell Mol Biol. 2006; 35:394–402. [PubMed: 16645180]
33. Chen BB, Mallampalli RK. Calmodulin binds and stabilizes the regulatory enzyme, CTP: phosphocholine cytidylyltransferase. J Biol Chem. 2007; 282:33494–33506. [PubMed: 17804406]
34. Zhou J, et al. Adenoviral gene transfer of a mutant surfactant enzyme ameliorates pseudomonas-induced lung injury. Gene Ther. 2006; 13:974–985. [PubMed: 16511521]
35. Bligh EG, Dyer WJ. A rapid method of total lipid extraction and purification. Can. J. Biochem. Physiol. 1959; 37:911–917. [PubMed: 13671378]
36. Folch J, Lees M, Sloane Stanley GH. A simple method for the isolation and purification of total lipides from animal tissues. J Biol Chem. 1957; 226:497–509. [PubMed: 13428781]
37. Kaewsuya P, Danielson ND, Ekhterae D. Fluorescent determination of cardiolipin using 10-N-nonyl acridine orange. Anal Bioanal Chem. 2007; 387:2775–2782. [PubMed: 17377779]
38. Mallampalli RK, Ryan AJ, Salome RG, Jackowski S. Tumor necrosis factor-alpha inhibits expression of CTP:phosphocholine cytidylyltransferase. J Biol Chem. 2000; 275:9699–9708. [PubMed: 10734122]

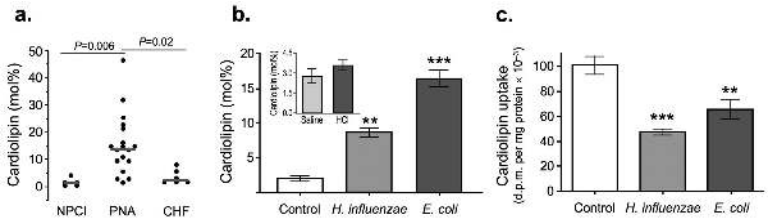

Figure 1. Quantification of cardiolipin (CL) in pneumonia

a. Panel a depicts the median (gray line) and distribution (black circles) of CL levels in tracheal aspirates from subjects with non-pulmonary critical illness (NPCI, *n*=five), pneumonia (PNA, *n*=17), and congestive heart failure (CHF, *n*=six). Groups were compared by Kruskal Wallis test (*P*=0.0007) followed by post hoc Wilcoxon Rank Sum analysis with Bonferroni correction for multiple testing **b.** C57BL/6 mice (three control, five *H. influenzae*, four *E.coli*) were infected intratracheally (i.t.) with *E. coli* (1×10^6 CFU/mouse) or *H. influenzae* (2×10^8 CFU/mouse). Mice were euthanized 48 h (*E. coli*) or 72 h (*H. influenzae*) later, lungs lavaged, and processed for CL assay. Inset: Mice (six/group) were given HCL (pH 1.5, 2 ml/kg i.t.) prior to being euthanized 30 min later for analysis of CL. **c.** Primary type II lung epithelia (from *n*=ten mice) were cultured with [^{3}H]-CL containing the commercial surfactant, Infasurf, for 2 h at 37 °C in the presence or absence of *E. coli* (MOI=100) or *H. influenzae* (MOI=10) and cellular CL uptake was determined. In (**b-c**), ** represents means ± S.D. with *P*<0.01, and *** represents *P*<0.001 vs. control as determined by one-way ANOVA analysis.

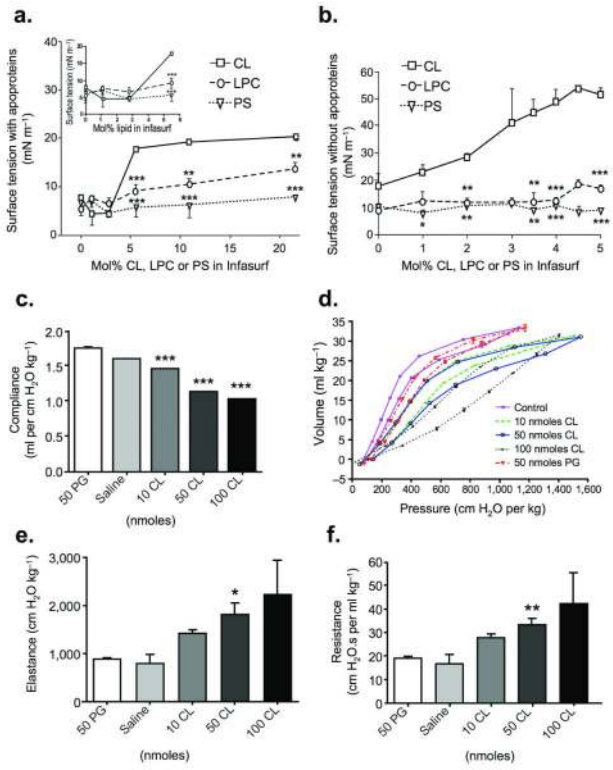

Figure 2. Biophysical effects of CL. a-b. Surface-tension

Cardiolipin (CL), lysophosphatidylcholine (LPC), and phosphatidylserine (PS) were reconstituted with Infasurf (liposomes in $CaCl_2$ (5 mM)) with apoprotein (**a**) or without apoprotein (**b**) and dynamic surface tension (γ_{min}) was measured using a pulsating bubble surfactometer. Increasing amounts of CL in Infasurf resulted in significantly increased surface tension compared to LPC or PS (magnified in inset). **c-f.** Mice (three-five/group) were anesthetized, paralyzed, and mechanically ventilated with a PEEP=3 and compliance (**c**), quasi-static pressure-volume curves (**d**), elastance (**e**), and resistance (**f**) was determined using a FlexiVent system after i.t. application of phosphatidylglycerol (PG) or CL. Significance was determined by a one-way ANOVA analysis where $^{*}P<0.05$, $^{*}P<0.01$, $^{***}P<0.001$ vs. control.

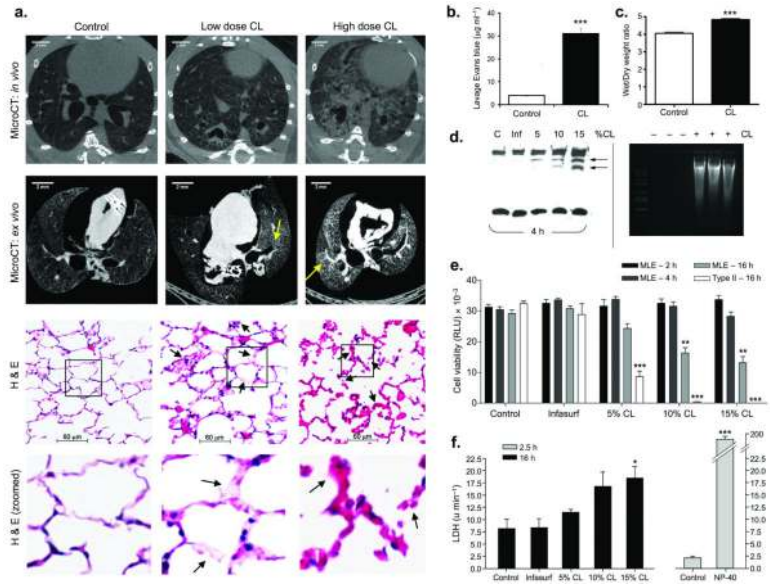

Figure 3. CL disrupts lung structure and alters epithelial cell viability

a. MicroCT scan images were obtained on live mice (*in vivo*) 1 h after i.t. administration of CL (50 nmole, [low], 100 nmole [high]) vs. control mice (above panels). In separate studies, mice were given CL as above and lungs were fixed and processed for microCT scanning (*ex vivo*). Data represents two mice/group. Below, third row: fixed tissue was processed for H & E staining (20× magnification). Lower row (middle) shows a high magnification (100×) image of foamy cells. **b-c.** CL induces lung edema. Mice were deeply anesthetized and administered CL (15 mM in 50 μl saline, i.t.; n = three) or vehicle (50 μl saline; n = 3). 30 min after CL administration Evan's Blue dye was injected intravenously. Wet/dry weights of lungs were also determined (c). $^{***}P<0.01$ vs. control. **d.** Primary mouse type II cells were serum starved for 24 h and then exposed to Infasurf (120 nmol/ml) or CL (5-15 Mol%) for various times prior to harvest for detection of poly(ADP-ribose) polymerase (PARP) cleavage (**d**, arrows, left panel); mice were also given i.t. CL (50 nmol) for analysis of lung DNA fragmentation using a DNA ladder extraction kit ([BioVision], **d**, right panel) or assayed for cell viability (**e**) and LDH release (**f**, primary type II cells). NP-40 was used as a positive control for LDH release. Data represents three separate experiments where $^{*}P<0.05$, $^{**}P<0.01$, and $^{***}P<0.001$ vs. control as determined by one-way ANOVA analysis.

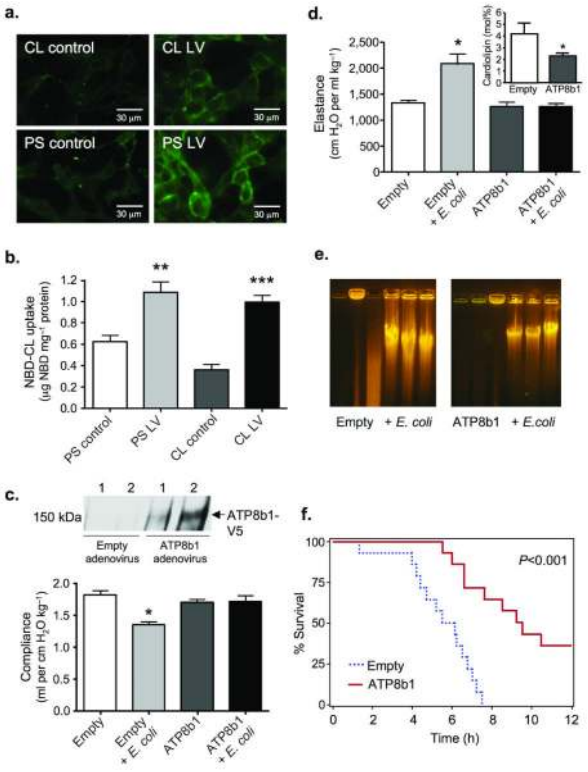

Figure 4. ATP8b1 overexpression

a-c. A lentiviral transduced V5-ATP8b1 stable cell line was labeled with NBD-CL or NBD-PS and cells were processed for fluorescence uptake by time-lapse microscopy. The lentiviral transduced ATP8b1 cell line exhibited increased uptake of NBD-labeled CL and NBD-labeled PS compared to untransduced control cells as quantitated by fluorescence spectrophotometry in (b). $^{**}P<0.05$ and $^{***}P<0.001$ by an unpaired t test. **c-d.** Mice (eight/group) received an empty vector (Ad5) or Ad5-ATP8b1 (2.5×10^8 PFU) i.t. and 24 h later given *E. coli* at 10^6 CFU/mouse for 48 h. Animals were anesthetized, paralyzed and mechanically ventilated and lung mechanics determined as in Fig. 2. The data in (**c**) top panel is a representative immunoblot showing levels of V5-immunoreactive ATP8b1 in lung tissue from two mice receiving Ad5 or Ad5-ATP8b1. In (**d**) CL levels were assayed in BAL after Ad5-ATP8b1 or Ad5 infection. Significance was determined by a one-way ANOVA where in (**c**) and (**d**) $^{*}P<0.05$ for empty + *E. coli* vs. other groups. **e**. Mice treated as in (**c**) were also analyzed for lung DNA fragmentation. **f**. Kaplan-Meier survival curve for mice infected with Ad5 empty or Ad5-ATP8b1 and infected with *E. coli*. (5×10^6 cfu/mouse, n=14 mice/group, $P<0.001$, log rank test).

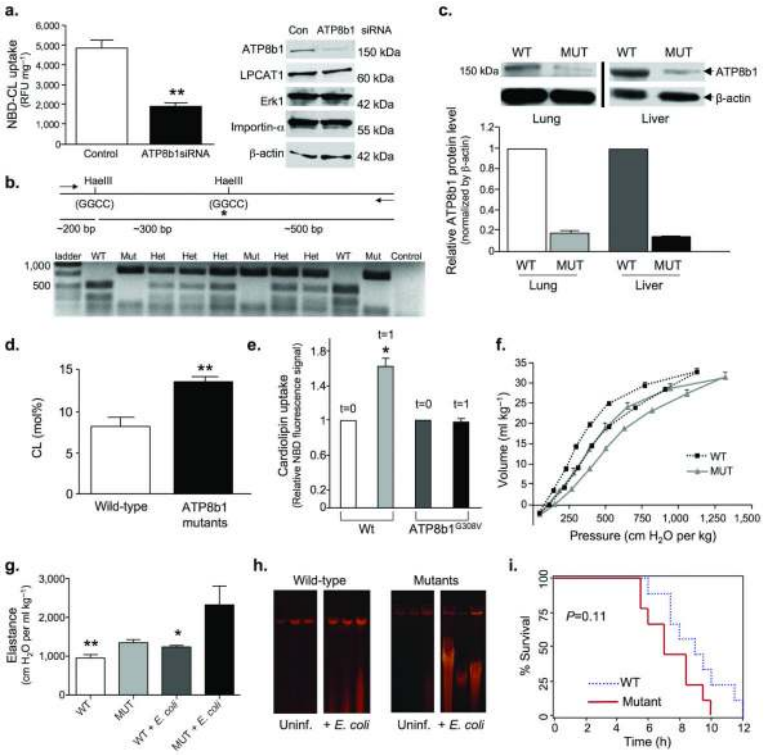

Figure 5. ATP8b1 defective mice are prone to bacterial-induced lung injury

a. ATP8b1 siRNA knockdown. Human A549 ATII cells were transfected with ATP8b1 siRNA or control RNA and incubated with NBD-labeled CL or PS for 30 min at 37 °C prior to harvest for uptake (left) and immunoblotting (right) using 25 μg of protein loaded/lane. Blots were probed with ATP8b1, LPCAT1, Erk1, importin-α, and β-actin antibodies. $^{**}P<0.01$. **b**. ATP8b1$^{G308V/G308V}$ mutants genomic DNA has a Hae III restriction site (GGCC) in which the second G is mutated to T (glycine to valine) and is not recognized in restriction digests. Mutant genomic DNA generates an 800 bp fragment upon HaeIII digestion compared to a 500 bp fragment with wild-type genomic DNA. The HaeIII digestion pattern was used for genotyping wild-type (Wt), heterozygous (Het), and mutant (Mut) mice. **c.** ATP8b1 immunoblotting in mouse tissues. Below: densitometric analysis from *n*=six mice/group. **d.** CL was assayed in lung lavage from ATP8b1 mutant and wild-type littermates (three/group). $^{**}P<0.01$. **e**. Primary type II epithelia isolated from mutants or wild-type littermates (five mice/group) were incubated with NBD-CL and cellular uptake was assayed initially after labeling (*t*=0) and after 1 min. **f-g.** Mutants and wild-type littermates uninfected or infected (seven/group) with *E. coli* at 10^6 CFU/mouse for 48 h were analyzed for lung mechanics. Mice were mechanically ventilated for determination of quasi-static volume-pressure curves (**f**, [uninfected]), and elastance (**g**). Statistical significance was determined by a one-way ANOVA where in (**g**) ** WT vs. MUT + *E.coli*, $P<0.01$ and * WT+ *E. coli* vs. MUT+ *E. coli*, $P<0.05$. **h**. Wild type and mutant mice treated as in (**g**) were also analyzed for lung DNA fragmentation. **i**. Kaplan-Meier survival curve for wild-type and ATP8b1 defective mice infected with *E. coli*, (5×10^6 CFU/mouse, seven mice/group, P=0.11, log rank test).

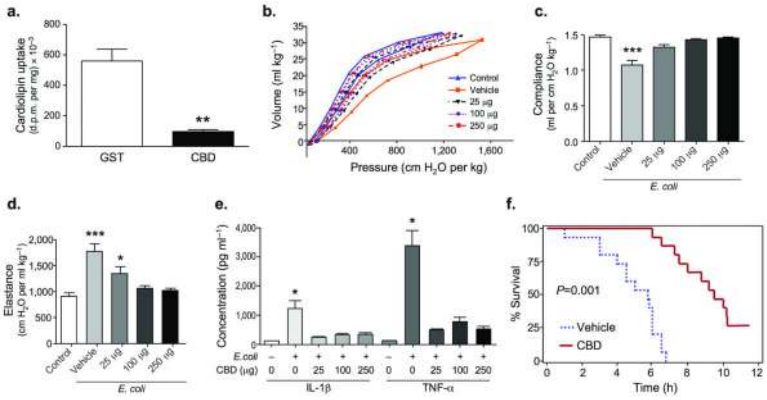

Figure 6. Cardiolipin binding domain (CBD) peptide blocks bacterial lung injury

a. ATP8b1 CBD-GST fusion peptide (CBD) or GST (control) were purified and incubated with MLE cells (10 µg of GST peptide or GST-CBD peptide/dish) in serum-free medium after labeling for 2 h with [^{3}H]-CL. Cells were harvested and processed for cellular [^{3}H]-CL uptake, $^{**}P<0.01$. **b-d.** C57/BL6 mice (six mice/group) were uninfected (control) or given *E. coli* at 10^6 CFU/mouse. After 48 h, mice were given vehicle, or CBD peptide into lungs using an aerosolizer. After 10 min, biophysical measurements were taken. Mice were mechanically ventilated for determination of quasi-static volume-pressure curves (**b**), compliance (**c**), and elastance (**d**). Significance was determined by a one-way ANOVA where in panel (**c**) $^{***}P<0.001$ vehicle vs. all other groups, (**d**) $^{*}P<0.05$ for 25 µg vs. either control or vehicle and $^{***}P<0.001$ vehicle vs. control, 100 µg, or 250 µg. (**e**). Mice (*n*=four/group) were inoculated with 1×10^6 CFU *E. coli* or uninfected for 48 h prior to i.t. administration of CBD. Mice were lavaged, and BAL supernatant assayed for cytokines. All *P* values are <0.05 for vehicle buffer + *E. coli*. (0+) vs. other groups**. f**. Kaplan-Meier survival curve for mice given i.t. CBD peptide (100 µg) and infected with *E. coli*, (5×10^6 CFU/mouse, *n*=14 mice/group, *P*=0.001, log rank test).